

1 A meta-Gaussian distribution for sub-hourly 2 rainfall

3 Marie Boutigny^{1,2}, Pierre Ailliot^{1*}, Aurore
4 Chaubet², Philippe Naveau³ and Benoît Saussol¹

5 ¹Laboratoire de Mathématiques de Bretagne Atlantique, UMR
6 6205, Université de Brest, France.

7 ²SPL Eau Du Ponant, Brest, France.

8 ³Laboratoire des Sciences du Climat et de l'Environnement,
9 EstimR, LSCE/IPSL, CNRS-CEA-UVSQ, Université
10 Paris-Saclay, Gif-sur-Yvette, France.

11 **Abstract**

12 Meta-Gaussian models are ubiquitous in the statistical literature. They
13 provide a flexible building block to represent non-Gaussian distributions
14 which inherit modeling and inference methods available in the Gaussian
15 framework. In particular they have been widely used for modeling rainfall
16 distributions. The first step when working with meta-Gaussian models
17 consists in choosing an appropriate transformation which allows to map
18 the Gaussian distribution to the target rainfall distribution. Many trans-
19 fer functions have been proposed in the literature but most of them are
20 not appropriate to describe heavy-tailed distributions, which is known to
21 be a usual feature for rainfall at sub-daily scales. In this context, we pro-
22 pose and study a new meta-Gaussian model that can handle heavy-tailed
23 observations. It leads to a four parameter model for which each param-
24 eter is linked to a different part of the distribution: a first one describes
25 the probability of rainfall occurrence, two of them are related to the lower
26 and upper tailed features of the distribution, and the last one is just a
27 scaling parameter. Theoretical arguments are given to justify the pro-
28 posed model. A statistical analysis of seven French rain gauges indicates
29 the flexibility of our approach under different climatological regions and
30 different aggregation times, here from six minutes to twenty four hours.
31 Our distribution outperforms other meta-Gaussian models that
32 have been proposed in the literature and, in particular, it
33 captures well heavier tail behaviours below the hourly scale.

2 *A meta-Gaussian distribution for sub-hourly rainfall*

34 **Keywords:** Rainfall distribution, meta-Gaussian model, heavy-tailed
 35 distributions

36

1 Introduction

37 Precipitation intensities and frequencies are key variables for many environmental
 38 studies, not only in hydrology but also agronomy, meteorology and
 39 impact studies (see e.g. [1], [2]). As a consequence, there is an abundant literature
 40 on the modeling of daily and monthly rainfall intensity distributions
 41 at a single location. The most popular distribution for positive daily precipitation
 42 is probably the gamma distribution [3], which also generally provides
 43 an adequate fit for precipitation at the monthly scale. Other distributions
 44 have been proposed such as the mixed exponential [4], Weibull [5] and log-
 45 normal [6]. Comparisons were made for specific data sets. For example, [7]
 46 ranked the mixed exponential first and the gamma second whereas [8] ranked
 47 the log-normal first, then mixed exponential, gamma and finally exponential.
 48 The performance strongly depends on the location of interest as local climate
 49 strongly impacts rainfall distribution.

50 The meta-Gaussian framework is the most usual strategy to construct multivariate
 51 models for rainfall distributions. The building block of this approach
 52 is to link the phenomena of interest to a Gaussian distribution. A common
 53 justification behind all these Gaussian based transformation techniques is that
 54 the normal distribution represents a solid, simple and flexible building block
 55 to construct multivariate models and handle for example space-time data [9].
 56 Furthermore it allows to model simultaneously the occurrence (dry/wet measurement)
 57 and amount of precipitation by censoring the Gaussian variable. As
 58 a consequence, meta-Gaussian models have been widely used in the literature
 59 on rainfall disaggregation [10–12], downscaling and model correction [13–15],
 60 short term or spatial prediction [16, 17], building stochastic weather generators
 61 [18–20], data assimilation [21], post-processing precipitation forecasts [22]
 62 or merging different data sources [23].

63 One key ingredient of meta-Gaussian model is the choice of an appropriate
 64 transformation to map a Gaussian distribution into a distribution relevant
 65 to describe the phenomenon of interest. The most usual transformation in the
 66 statistical literature is probably the Box-Cox transformation [24] which has
 67 also been applied for rainfall [9, 23]. Other transformations have been proposed
 68 for modeling rainfall specifically, such as the square root transformation
 69 in [25], power transformations [18] or power exponential [12]. Another strategy
 70 is to use a transformation based on cumulative distributions and quantile functions,
 71 which maps the Gaussian distribution to a target distribution such as
 72 the gamma distribution ([20]) or the mixed exponential distribution [26], but
 73 this generally leads to transformations with relatively complicated analytical
 74 expressions.

A particular impetus for this work was the need to describe rainfall distributions at fine time scales (a few minutes) in order to test the sensitivity and robustness of an urban hydrological model in Brest (France). At sub-hourly scales, rainfall measurements are frequently null (when no rain is measured) and discrete due to rain gauge precision. Still, very few events with high intensities strongly skew the density to the right, creating a heavy tailed distribution which needs to be treated with care. The models described above do not produce heavy-tailed distributions and thus may not be appropriate for describing sub-hourly precipitations. More generally, the statistical modeling of the distribution of rainfall accumulated over short time periods is little discussed in the literature.

Extreme value theory promotes the use of the Generalized Pareto distribution (GPD) for modeling exceedances over a high threshold [27, 28]. One difficulty with this approach is that only exceedances above a high threshold are modelled, not the full distribution. Hybrid distributions were proposed in this context [29]. For example, [30] propose a meta-Gaussian model where a Gamma distribution is used to describe low and moderate rainfall, i.e. rainfall below a fixed threshold, and the GPD is used to describe rainfall above the threshold. However, finding the optimal threshold that allows the use of a GPD for the exceedances remains a delicate task for the practitioner. Different methods have been proposed to bypass the threshold selection step. In particular, [31] proposed the Extended GPD model. This leads to a flexible model which can describe the full rainfall distribution range and handle heavy tails. In contrast to a meta-Gaussian model, this approach is based on the uniform distribution, not the Gaussian one. So, this may bring some complexity in some types of extensions, see [32]. In addition, it does not handle dry events.

The main contribution of this paper is to propose a new meta-Gaussian model which is simple but flexible enough to model the full rainfall distributions accumulated over a wide range of time scales including dry, low and heavy precipitations. The paper is organised as follows. The data sets that will be used throughout the paper are introduced in Section 2. The proposed model is introduced in Section 3, together with some theoretical justifications. Section 4 discusses results obtained when fitting the model to the data. Finally conclusions and perspectives are given in Section 5.

All the models discussed in this paper can be fitted with the R package available on Github at <https://github.com/mbtgy/tcG>.

2 Data

In this study, we consider rainfall data recorded at 7 meteorological stations in France represented on Figure 1. These data were provided by Météo-France. They are available at a 6 minutes time step from 2010 until 2021 (12 years). In order to remove seasonal components, a focus is made on the three months of summer, i.e. June, July and August where the more intense convective

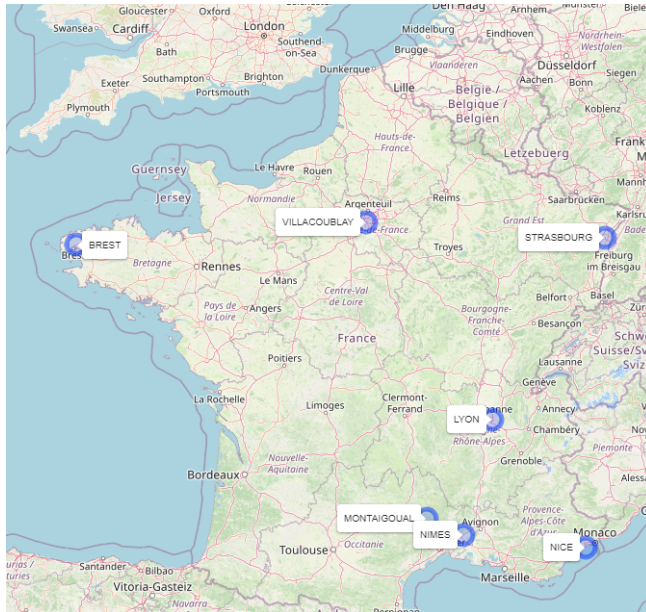
4 *A meta-Gaussian distribution for sub-hourly rainfall*

Fig. 1 Locations of our seven rain gauge Metep France stations in France with a six minute time scale recording from 2010 to 2021 (summer months). Different sites correspond to different climates. For example, the westernly climate in the Brittany peninsula strongly differs from the drier southern Mediterranean one.

117 precipitation events generally occur. All the data were measured using tipping
 118 bucket gauges with a 0.2 mm precision.

119 This work was triggered by the need of high resolution space-time data
 120 which can be used as input of an urban hydrological model which describes
 121 the sewage system of the city of Brest. One difficulty when trying to merge
 122 the different sources of rainfall data available over a particular geographical
 123 area such as the watershed of the city of Brest is that they are generally avail-
 124 able at different time steps. For example, recent rain gauge typically provide
 125 measures of the precipitation accumulated over 3 or 6 minutes, whereas his-
 126 torical measurements are only available at the hourly or daily scale. Other
 127 sources of data such as radar, satellite or model outputs may also be available
 128 at other time resolutions. In such situation, it is useful to have a simple para-
 129 metric model which can describe the distribution of precipitation at different
 130 time resolutions ranging from a few minutes to daily data. We also consider
 131 6 other stations, located in different climate zones (continental, mountainous
 132 and Mediterranean), to check the flexibility of the proposed model.

133 Figure 2 shows that the temporal resolution has a strong influence on the
 134 shape of the rainfall distribution in Brest. Obviously, the percentage of dry
 135 records decreases with the duration over which rainfall is accumulated: for 6-
 136 minutes data, the percentage of dry measurements is equal to 96.7% whereas
 137 it drops to 31.6% for daily data. The empirical distribution of the 6-minutes
 138 data (left panel) is highly skewed, with a majority of positive records being

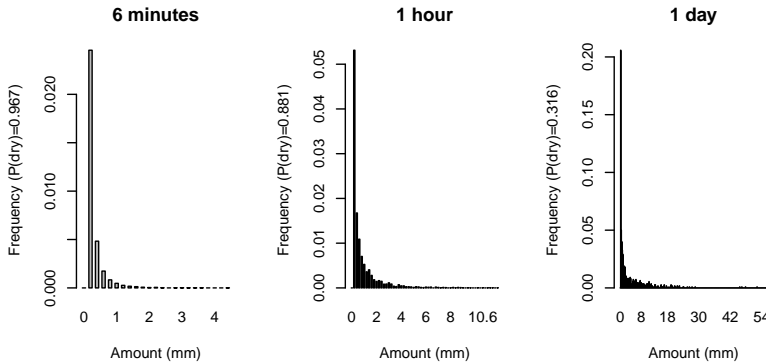


Fig. 2 Empirical distribution of rainfall accumulated over 6 minutes (left), 1 hour (middle) and 1 day (right) in Brest. Dry measurements are not represented but the percentage of dry measurements is indicated in the y-label.

139 equal to the 0.2 mm precision of the tipping bucket, but also high values corre-
 140 sponding to intense convective events, which creates a heavy tail distribution.
 141 The empirical distributions of hourly (middle panel) and daily (right panel)
 142 rainfall are also skewed, but it is less pronounced than for 6-minutes data.

143 Also note that the 0.2 mm precision of the tipping bucket leads to a dis-
 144 cretization of the (continuous) distribution of the rainfall. This discretization
 145 is clearly visible when looking at the empirical distribution of the 6-minutes
 146 rainfall data, whereas it becomes less prominent when looking at hourly or
 147 daily data. This has to be taken into account when fitting the continuous model
 148 introduced in the next section to the data (see Section 4.1).

149 To sum up, the goal is to develop a simple parametric model which can
 150 describe the distribution of precipitation at different time scales, hence to have
 151 a strongly skewed distribution with a discrete component in zero and the ability
 152 to produce heavy tails. The next section discusses the choice of such model.

153 3 Model

154 3.1 Meta-Gaussian models

A classical approach for modeling rainfall, sometimes called meta-Gaussian model, is to assume that rainfall amounts Y can be linked to a Gaussian variable X with mean μ and variance 1 according to

$$155 \quad Y = \psi(X) \mathbb{1}_{X \geq 0}, \quad \text{with } X \sim \mathcal{N}(\mu, 1), \quad (1)$$

where $\psi : [0, +\infty[\rightarrow]0, +\infty[$ is an increasing function which is generally referred to as the anamorphosis in the literature and $\mathbb{1}_{X \geq 0}$ is the indicator function equal to 1 if condition $X \geq 0$ is true and 0 otherwise. The operation of such model is schematised in Figure 3. The censorship in 0 produces dry conditions

6 *A meta-Gaussian distribution for sub-hourly rainfall*

(step 1 in Figure 3) with a proportion linked to the mean of the Gaussian according to

$$P(Y = 0) = P(X \leq 0) = \Phi(-\mu)$$

155 where Φ is the cumulative distribution function (cdf) of the standard normal
 156 distribution. The transformation ψ acts on the positive part of the distribution
 157 which corresponds to wet conditions (step 2 in Figure 3).

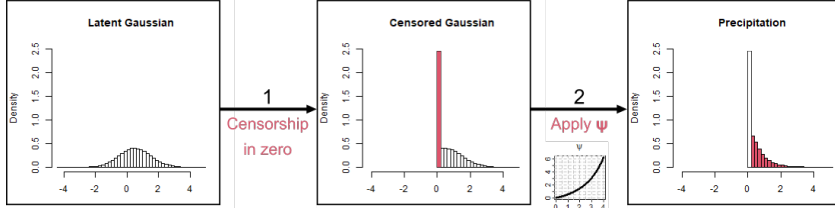


Fig. 3 Schematic functioning of a meta-Gaussian model. The coloured areas in the histograms represent the part of the distribution modified at each step.

The cdf of the random variable Y defined by (1) can be written as

$$F(y) = \begin{cases} \Phi(\psi^{-1}(y) - \mu) & \text{if } y > 0 \\ \Phi(-\mu) & \text{if } y = 0 \end{cases}. \quad (2)$$

Remark that this meta-Gaussian model is general since any positive random variable with a discrete component at the origin like precipitation can be written as (1) using

$$\psi(x) = F^{-1}(\Phi(x - \mu)) \quad (3)$$

where $\mu = -\Phi^{-1}(P(Y = 0))$ and F^{-1} denotes the quantile function (generalized inverse function of the cdf F) of Y . Plugging a non-parametric estimate of the quantile function F^{-1} in (3) allows building non-parametric estimates of ψ , [?] see, e.g., lien2013effective, cecinati2017comparing. The dots in Figure 4 show the estimate obtained on the 6-minutes rainfall data in Brest introduced in Section 2. The shape of ψ near zero is linked to the small precipitations. A horizontal tangent at the origin means that they are more low rainfall than expected low values in the censored Gaussian distribution and the density becomes more concentrated in 0 if ψ is flatter at the origin. The growth speed is linked to the upper tail: the convex-exponential shape indicates that the tail is heavier than a Gaussian one. However, parametric approaches are generally favoured in the applications and many models have been proposed for ψ in the literature. The most classical one is probably the power transformation, see [18] and [16],

$$\psi(x) = \sigma x^{1/\alpha}, \quad (4)$$

but other transformations have been proposed. [11] studied a quadratic power function, [14] worked with a simple exponential transform and [12] focused on

$$\psi(x) = \sigma_2(\exp(\sigma_1 x^{1/\alpha}) - 1). \quad (5)$$

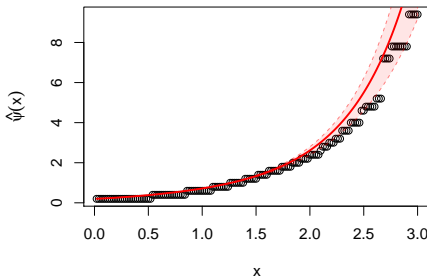


Fig. 4 Non-parametric estimate of the anamorphosis function based on (3) (dots) for the 6-minutes data in Brest-Guipavas. The plain curve corresponds to the parametric model (13) fitted to the data (see Section 4.1), and the dotted line is its 95% confidence interval computed using 500 bootstrap samples.

To force the resulting distribution to match a specific distribution the inverse of a cdf can also be used, as it is the case with the Gamma distribution in [20].

Transformation (4) being the most commonly used, it will be a point of comparison and will be referred to as the classical meta-Gaussian model. Note that it is closely related to the popular Box-Cox transformation [24].

3.2 Lower and upper tails of meta-Gaussian models

The choice of an appropriate anamorphosis function for a particular application is typically a trade-off between model complexity, versatility, tractability and interpretability. In this section, it is advocated that the properties of lower and upper tails of the positive part of the rainfall distribution may also provide interesting insights.

Different studies have shown that rainfall at daily or sub-daily scales are generally heavy tailed [27]. In this situation, ψ should be chosen such that the transformed Gaussian variable defined by (1) is tail equivalent with a Pareto distribution with positive shape parameter ξ . According to B, this holds true if and only if

$$\lim_{x \rightarrow \infty} \frac{x\psi(x)}{\psi'(x)} = \frac{1}{\xi}. \quad (6)$$

Solving the differential equation $\frac{x\psi(x)}{\psi'(x)} = \frac{1}{\xi}$ leads to a first function $x \mapsto \exp \frac{\xi x^2}{2}$ which satisfies (6). Then, by re-writting ψ as

$$\psi(x) = \exp \frac{\xi x^2}{2} \exp u(x) \quad (7)$$

- which is always possible - condition (6) becomes

$$\lim_{x \rightarrow \infty} \frac{u'(x)}{x} = 0.$$

8 *A meta-Gaussian distribution for sub-hourly rainfall*

This condition seems easier to work with as it allows understanding that loosely speaking, the anamorphosis function ψ should increase "like" the function $x \mapsto \exp \frac{\xi x^2}{2}$ when $x \rightarrow +\infty$ to get heavy tailed distributions. In particular, one can check that most of the anamorphosis found in the literature - including the classical meta-Gaussian model (4) introduced previously - do not satisfy condition (6). Hence, these transforms are not particularly well suited to model heavy rainfall at small time scales. Interestingly, the model of [12] will be tail equivalent to a Pareto distribution if and only if $\alpha = \frac{1}{2}$ in (5). The Tukey g-and-h distribution, [33–35] [], defined as the random variable

$$\frac{\exp(gX) - 1}{g} \exp \frac{\xi X^2}{2}, \quad \text{with } X \sim \mathcal{N}(0, 1)$$

170 with h and g real parameters, may not always satisfy condition (6). In addition,
 171 it is not directly suited to include the dry event component at 0 and it lacks
 172 flexibility to describe the shape of the lower part of the rainfall distribution
 173 according to the discussion below.

Concerning non zero but low rainfall, [31] advocated, using arguments of the extreme value theory, that the lower part of the distribution of the positive amount should approximately follow a power-law, i.e. satisfy

$$\lim_{y \downarrow 0} \frac{F(y) - F(0)}{y^\alpha} = C$$

for some positive constant C and shape parameter $\alpha > 0$. In particular, the often used Gamma distribution with shape parameter α satisfies this constraint. These authors proposed and studied different families that meet this criterion. One can wonder if this constraint could also be enforced to the meta-Gaussian model defined by (2). A first order Taylor expansion of F around zero indicates that condition (6) holds true if and only if

$$\psi(x) = x^{\frac{1}{\alpha}} K(x) \tag{8}$$

174 with K such that $\lim_{x \downarrow 0} K(x)$ exists and is strictly positive. Most of the
 175 anamorphosis functions in the hydrological literature, including the classical
 176 meta-Gaussian model (4) correspond to the particular case where $K(x)$ is a
 177 constant function, and consequently they obey this constraint on low rainfall
 178 amount. Remark that the same parameter α in model (5) both controls the
 179 shape of the distribution for low and heavy rainfall. This is an undesirable
 180 property as is not impossible to create a heavy-tailed distribution with a power
 181 shape parameter different from $\alpha = \frac{1}{2}$ for low rainfall.

182 3.3 Proposed model

According to the previous section, the anamorphosis ψ should be chosen such that conditions (6) and (8) are satisfied in order to obtain a Meta-Gaussian

distribution with a Pareto upper tail and a lower tail that follows a power law. Based on these results, this paper advocates the use of the anamorphosis function

$$\psi(x) = \sigma x^{\frac{1}{\alpha}} \exp \frac{\xi x^2}{2} \quad (9)$$

with $\mu \in \mathbb{R}$, $\sigma \in \mathbb{R}^{+*}$, $\alpha \in \mathbb{R}^{+*}$ and $\xi \in \mathbb{R}$. The distribution of the random variable Y defined through (1) with $X \sim \mathcal{N}(\mu, 1)$ and ψ given by (9) will be referred to as the GP meta-Gaussian distribution with parameter $(\mu, \sigma, \alpha, \xi)$. μ is directly related to the dry probability through (2) and σ is a multiplicative scale parameter. ψ defined by (9) satisfies condition (8) and thus the lower tail of the positive part of the distribution has a power shape with shape parameter α . It also satisfies (6) and thus the upper tail distribution is controlled by the shape parameter ξ . More precisely, if $\xi > 0$, the distribution is tail equivalent with a Pareto distribution with shape parameter ξ . It implies in particular that $E[Y^p] = +\infty$ if $p > \frac{1}{\xi}$. The case $\xi = 0$ corresponds to the classical meta-Gaussian model (4). Negative values for ξ creates an upper bound to the distribution as for the GPD distribution. Indeed, when $\xi < 0$, ψ is strictly monotonic increasing only on the interval $(0, x_{sup})$ with

$$x_{sup} = \sqrt{\left| \frac{-1}{\min(\alpha\xi, 0)} \right|}. \quad (10)$$

The GP meta-Gaussian distribution is thus defined by applying (1) with ψ given by (9) to the Gaussian variable $X \sim \mathcal{N}(\mu, 1)$ truncated at x_{sup} . Remind that truncation means that values above x_{sup} are not observed - unlike the censorship that is used to create the dry component, where the observations above the bound take the value of the bound. The support of the distribution is $[0, y_{sup}]$ with

$$y_{sup} = \sigma \left(\frac{e^{-1}}{\max(-\alpha\xi, 0)} \right)^{\frac{1}{2\alpha}}$$

the upper bound in the precipitation domain. Note that when $\xi \geq 0$ the bounds become $x_{sup} = y_{sup} = +\infty$, so those notations can be used for $\xi \in \mathbb{R}$. When the Gaussian is truncated above x_{sup} , the cdf (2) must be corrected by the probability of truncation (see A).

An advantage of the GP meta-Gaussian transformation over other transformations which satisfy (6) and (8) is the possibility to derive an analytical expression for the inverse of ψ

$$\psi^{-1}(y) = \sqrt{\frac{1}{\alpha\xi} W \left(\alpha\xi \left(\frac{y}{\sigma} \right)^{2\alpha} \right)} \quad (11)$$

where W denotes the Lambert W function [34] defined as the inverse of the function $x \mapsto x \log x$. Note that the Lambert W function is available in usual statistical software which simplifies practical implementation of the model.

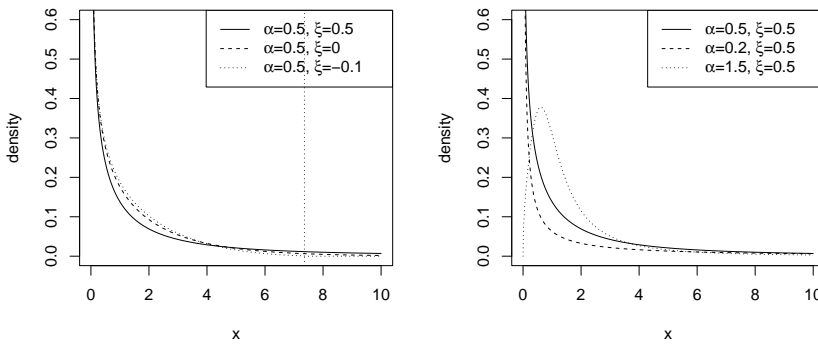


Fig. 5 Probability density function of the GP meta-Gaussian distribution for different parameter values. All the plots were obtained with $\mu = 0$ and $\sigma = 1$. The left panel shows the influence of ξ and the right panel the influence of α . The vertical dotted line on the left plot corresponds to the upper bound y_{up} of the distribution with $\xi = -0.1$. Only the positive part of the distribution is shown.

In particular, analytical expressions for the cdf and the probability density function (pdf) of the GP meta-Gaussian model can be derived from (2). This simplifies the computation of the likelihood function and the fitting the model to data (see Section 4.1 for more details). Analytical expressions for the finite moments can also be derived, which is not the case for many meta-Gaussian models that can be found in the literature (to the best of our knowledge the classical transform (4) is the only other meta-Gaussian model with analytical moments). Expressions for the pdf, cdf, quantile function and moments of the GP meta-Gaussian model can be found in A.

Figure 5 illustrates the flexibility of the GP meta-Gaussian distribution with different parameter values. The distribution with $\mu = 0$, $\sigma = 1$, $\alpha = 0.5$ and $\xi = 0.5$ is used as a reference since it corresponds to typical parameters values for the rainfall data considered in this study. The left panel shows that the parameter ξ influences the upper tail of the distribution whereas α modifies the shape of the distribution for low rainfall (see right panel) as expected from the theory.

206 4 Numerical results

207 4.1 Parameter estimation

208 This section describes the method used to fit the model introduced in the
 209 previous section to the data. As discussed in Section 2 (see also Figure 2) the
 210 functioning of a tipping bucket induces a discretization of the data which needs
 211 to be taken into account.

For that, we assume that

$$P(N = n) = P(n \leq Y < n + \delta) \quad (12)$$

212 where Y is the (not observed) continuous rainfall, N represents the (observed)
 213 discrete measurement with values in $\{0, \delta, 2\delta, \dots\}$ and δ denotes the precision
 214 of tipping bucket, i.e. 0.2 mm for our data sets.

Applying (12) with $n = 0$ gives

$$P(N = 0) = P(Y < \delta)$$

and thus with the anamorphosis (9) the probability of having a dry measurement depends not only on μ but also on the parameters $\{\sigma, \alpha, \xi\}$ of the anamorphosis function. This creates additional dependence between the different parameters and complicates the interpretation of the parameters. In order to get round this difficulty, the definition of ψ is modified as follows

$$\psi(x) = \delta + \sigma x^{\frac{1}{\alpha}} \exp \frac{\xi x^2}{2}. \quad (13)$$

215 Note that ψ^{-1} and y_{sup} are consequently modified. We found that the introduction
 216 of δ in the anamorphosis function greatly improves the results obtained
 217 when fitting the model to the data sets considered in this study.

In order to fit the GP meta-Gaussian model, the maximum likelihood approach is used in this study. When fitting a continuous distribution model to rain gauge data, the likelihood is usually computed directly from the continuous density. However it has been noticed that taking into account the discretization significantly improves the results. More precisely, the discrete log likelihood which is maximised is based on (12)

$$\log \mathcal{L}(\theta) = n_0 \log(\Phi(-\mu)) + \sum_{i: n_i > 0} \log \{F(n_i + \delta) - F(n_i)\} \quad (14)$$

218 where n_0 is the number of dry measurements, (n_1, \dots, n_n) the rainfall data,
 219 $\theta = (\mu, \alpha, \sigma, \xi)$ the unknown parameter and F the cdf of the distribution of Y
 220 (which depends on θ).

We found that the maximum likelihood estimates (MLE) obtained by maximising (14) over θ leads to estimates of α , σ and ξ which are strongly correlated together. The dependence between the estimates of σ and ξ is not surprising since it is well known that a similar behaviour occurs for the GPD distribution: the MLE of the scale and shape parameters are strongly dependent (see e.g. [36] and references therein). We also found a strong dependence between the MLE of α and σ , even when fitting the classical model (4) where $\xi = 0$. This is especially true when fitting the model to rainfall data at a sub-hourly time-step: the discretization has a strong impact (see Figure 2) and this may complicate the estimation of the lower-tail shape parameter α . The

12 *A meta-Gaussian distribution for sub-hourly rainfall*

existence of this dependence between the different estimates complicates the interpretation of the results. A usual method to overcome this problem (see e.g. [37]) is to add a penalty term in the likelihood. After some experimentation, we chose to maximise the following penalised log-likelihood function

$$\log \tilde{\mathcal{L}}(\theta) = \log \mathcal{L}(\theta) - \frac{(\alpha - 0.5)^2}{\tau^2}.$$

221 It favours estimates with a shape parameter α close to 0.5 and the hyperparameter
 222 τ controls the strength of the penalty. In the numerical results reported
 223 below, the value $\tau^2 = 0.001$ is used.

224

4.2 Results

225 In order to assess the flexibility and interpretability of the proposed GP Meta-
 226 Gaussian model, it was fitted to the rainfall data at the 7 meteorological
 227 stations represented on the map of Figure 1. For each of these stations, different
 228 temporal resolutions varying from 6-minutes to one day were considered,
 229 where lower resolution data are obtained by accumulating 6-minutes data over
 230 a longer time interval. In order to reduce the short-term temporal dependence
 231 in the data sets, one observation every k observations was retained for the
 232 analysis. The value of k depends on the time step between successive observa-
 233 tions, ranging from $k = 10$ for 6-minutes data, to $k = 5$ for 12-minutes data,
 234 $k = 2$ for 30-minutes data, and $k = 1$ if the time step is larger than 1 hour.

235 Figure 6 shows quantile-quantile plots for the fitted GP meta-Gaussian
 236 model at various time resolutions (6 minutes, 30 minutes, 1 hour and 1 day) for
 237 the 7 stations. The global fit of the model is very satisfying at all stations and
 238 time resolutions, except maybe for the smaller time steps in Lyon where the
 239 fitted model has difficulties in explaining the largest observation. It shows that
 240 the model is flexible enough to reproduce rainfall distributions for a variety of
 241 climates and temporal resolutions.

242 The classical meta-Gaussian model with power transformation (4) was
 243 also fitted to the data for comparison. Remind that this model is a partic-
 244 ular case of the GP meta-Gaussian model when the upper-tail parameter ξ
 245 is assumed to be equal to 0. The resulting quantile-quantile plots are super-
 246 imposed on Figure 6. The fits are generally less satisfactory than with the
 247 GP meta-Gaussian model, in particular regarding the upper-tail of the dis-
 248 tribution where the power transformation leads to an underestimation of the
 249 largest quantiles. This is not surprising since we know from the results given
 250 in Section 3.2 that it is not possible to produce heavy-tailed distributions with
 251 this model whereas rainfall data generally have heavy tails.

252 Figure 7 shows the evolution of the model parameters with time resolu-
 253 tion (note that the time axis is non linear). The evolution of the parameters
 254 is generally smooth. μ is increasing with aggregation, which is expected as
 255 there are less and less dry measurements when the period over which rainfall is
 256 accumulated increases. The estimate of the scale parameter σ is also generally

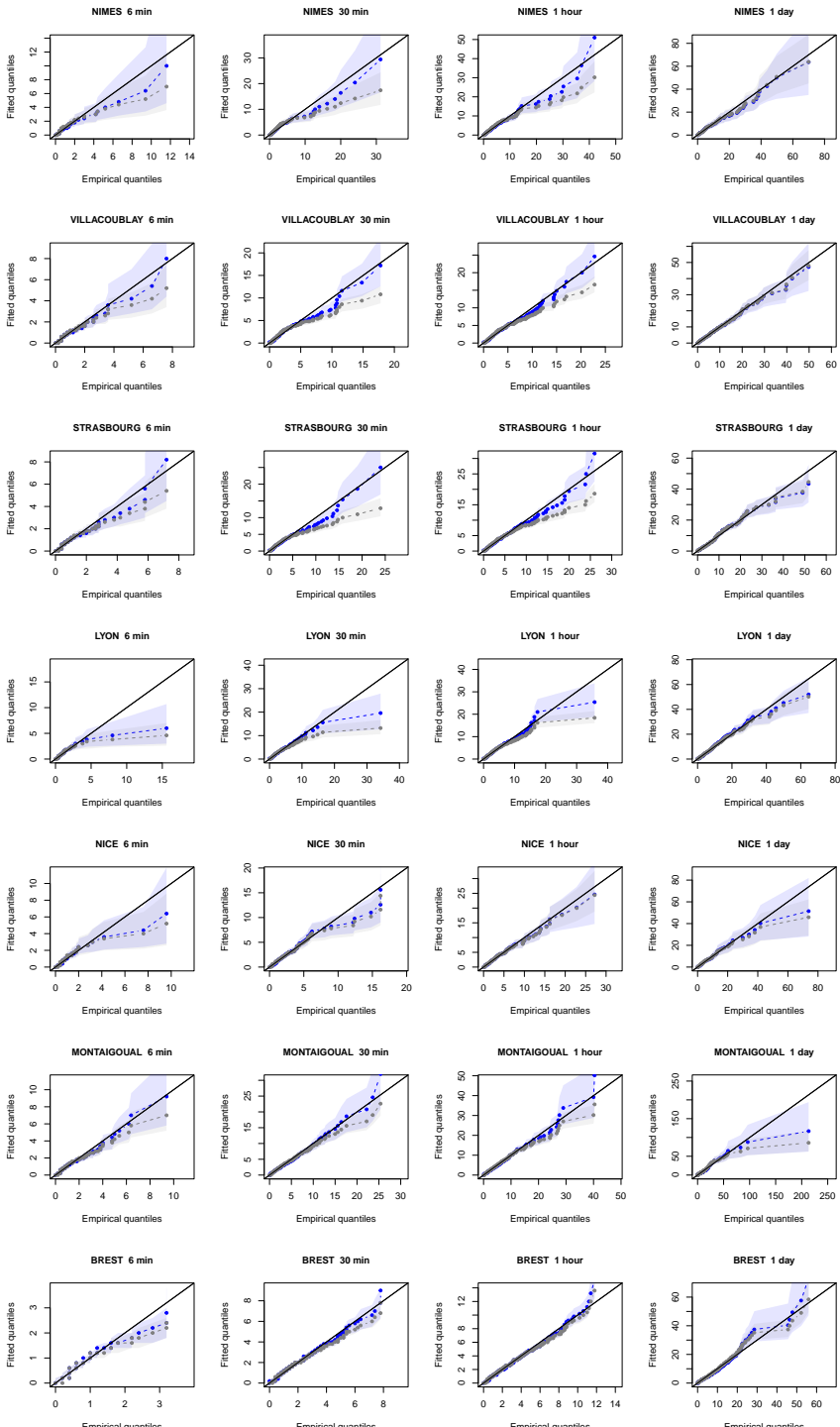


Fig. 6 Quantile-quantile plots for the GP (9) (blue) and power (4) (grey) meta-Gaussian models fitted to the rainfall data. Each column corresponds to a different time resolution and each row to a meteorological station. The light area gives (pointwise) 95% intervals based on 500 non parametric bootstrap replicates.

14 *A meta-Gaussian distribution for sub-hourly rainfall*

increasing, which is expected with the sum of (positively correlated) random variables. Remark however that there are some exceptions (e.g. Brest for larger time resolution) which may be due to the correlation between the estimates of σ and the other parameters. As concerns the upper tail parameter ξ , we generally obtain positive values (i.e. heavy-tailed distributions) but the evolution with time resolution seems to be site-dependent. For Nimes, Villacoublay, Strasbourg and Lyon (top panels of Figure 7), the estimated tail parameter ξ is relatively high for 6-minutes data and then decreases when rainfall is accumulated over longer time intervals. This is coherent with the intuition that summing random variable will tend to "gaussianize" them and produce distributions with lighter tails. However, for Nice, Montaigoual and Brest, a different behaviour is observed: the estimated tail parameter ξ is smaller for 6-minutes data and does not clearly decrease with the time resolution. The evolution of the lower tail parameter α is also site dependent. At some stations (Lyon, Strasbourg, Nimes, Villacoublay and Brest) it tends to increase and then decrease with a maximum value reached for hourly data, whereas it is the opposite at Montaigoual. Remind that lower values of α lead to a distribution which is more more "peaky" at the origin. The explanation behind this temporal evolution is not straightforward. The rainfall accumulated over a given time period is the sum of a random number (because of the dry measurements) of correlated (because of the temporal dependence) random variables and hence it may have a complicated behaviour. It thus depends on the climate of the different stations, the characteristics of the rainy events in terms of intensity and duration impacting the distribution of the accumulated rainfalls.

281

5 Conclusions and perspectives

282 In this work, we propose a new meta-Gaussian distribution with four parameters that can handle heavy-tailed data with a discrete component at the origin. The proposed GP meta-Gaussian model is tractable and analytical expressions exist for the pdf, cdf, quantile function and for the moments.

286 It was found that the model is flexible enough to describe the distribution
 287 of rainfall over a variety of climates and time resolutions. Comparison with a
 288 classical meta-Gaussian model shows what the proposed transform brings to
 289 this class of models: a better fit at small time scales due to its capacity to pro-
 290 duce heavy tails. The GP meta-Gaussian model is quite similar to the extended
 291 GP model [31] in terms of construction but also in terms of performance. The
 292 advantage of the meta-Gaussian model is its direct link with a Gaussian vari-
 293 able that allows the use of methods developed for Gaussian data (multivariate,
 294 spatiotemporal models, Kalman-like algorithm, etc.) and also the possibility
 295 to easily include the discrete component associated to dry conditions.

296 It was also found that the parameters of the model evolves smoothly
 297 with temporal resolution. This could be useful for example to extrapolate the
 298 parameters and thus "estimate" the distribution of the rainfall at unobserved
 299 time resolution. However, much works remain to be done to understand how

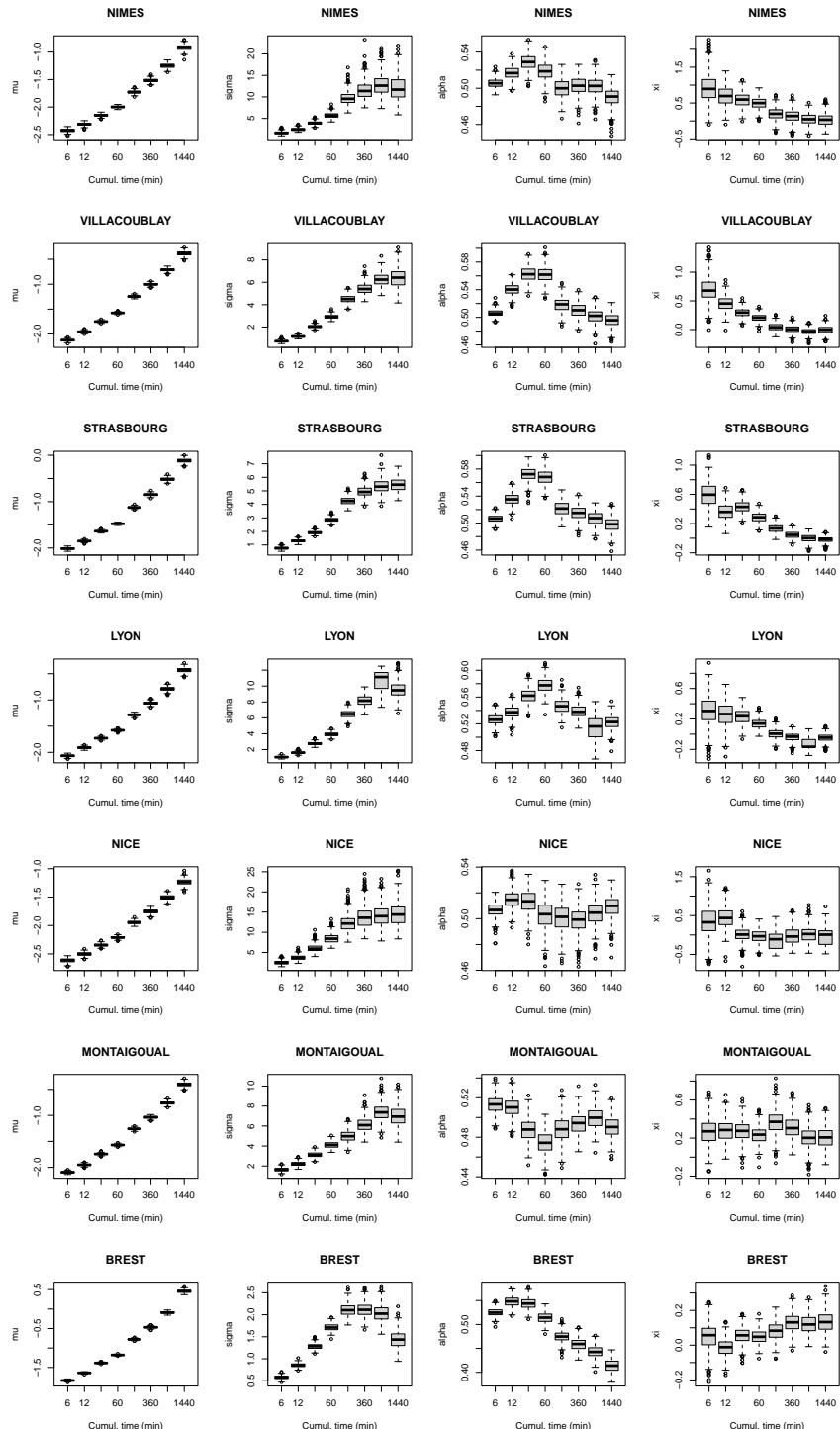


Fig. 7 Parameters estimates of the GP meta-Gaussian model fitted to the data at various time resolution. Each column corresponds to a different parameter of the GP meta-Gaussian and each row to a meteorological station. The boxplots are based on 500 non parametric bootstrap replicates.

300 the temporal dynamics of the dry and rainy events impacts the distribution
 301 of the rainfall accumulated at different temporal resolutions. This will be the
 302 topic of future work, with the aim to derive a temporal model compliant with
 303 the properties of rainfall at different time scales. Another possible extension
 304 is to adapt this meta-Gaussian distribution to spatial rainfall structures, in
 305 particular to improve regional frequency analysis, see e.g. [38] and [39].

306 **Appendix A Some Theoretical Properties of
 307 the GP Meta-Gaussian
 308 Distribution**

The density, cdf and quantile function of a meta-Gaussian model as defined in (1) are

$$f(y) = c \times \begin{cases} \phi_\mu(\psi^{-1}(y))/\psi'(\psi^{-1}(y)) & \text{if } y > 0 \\ \Phi_\mu(0) & \text{if } y = 0 \end{cases},$$

$$F(y) = c \times \begin{cases} \Phi_\mu(\psi^{-1}(y)) & \text{if } y > 0 \\ \Phi_\mu(0) & \text{if } y = 0 \end{cases},$$

$$F^{-1}(u) = \begin{cases} \psi(\Phi_\mu^{-1}(u/c)) & \text{if } u > \Phi_\mu(0) \\ 0 & \text{if } u = \Phi_\mu(0) \end{cases},$$

309 with ϕ_μ and Φ_μ denoting respectively the pdf and cdf of a normal distribution
 310 with mean μ . c is the normalisation constant that deals with the probability
 311 of truncation when $\xi < 0$ with the GP meta-Gaussian transform. Hence $c = 1$
 312 for the classical transform (4), and for the GP meta-Gaussian transform
 313 (9) $c = 1/\Phi_\mu(x_{sup})$, with x_{sup} the upper bound in the Gaussian domain as
 314 defined in (10).

315

An explicit expression of the moments was found for the GP meta-Gaussian distribution when $\xi \geq 0$. Let us write Y_+ the wet measurements.

$$E(Y_+^p) = \frac{1}{\sqrt{2\pi}(1 - \Phi(-\mu))} \int_0^{+\infty} \psi(x)^p \exp\left\{-\frac{1}{2}(x - \mu)^2\right\} dx$$

$$= \frac{\sigma^p}{\sqrt{2\pi}(1 - \Phi(-\mu))} \exp\left(-\frac{\mu^2}{2}\right) \int_0^{+\infty} x^{p/\alpha} \exp\left\{-\frac{1 - \xi p}{2}x^2 + \mu x\right\} dx$$

By identification in [40] (eq. 3.462.1, page 365), with $\gamma = -\mu$, $\nu - 1 = p/\alpha$ and $\beta = (1 - \xi p)/2$,

$$E(Y_+^p) = \frac{\sigma^p(1 - \xi p)^{-\frac{1}{2}(\frac{p}{\alpha} + 1)}}{\sqrt{2\pi}(1 - \Phi(-\mu))} \exp\left\{\frac{\mu^2}{2} \left(\frac{1}{2(1 - \xi p)} - 1\right)\right\} \Gamma\left(\frac{p}{\alpha} + 1\right) D_{-(\frac{p}{\alpha} + 1)}\left(-\frac{\mu}{\sqrt{1 - \xi p}}\right)$$

316 Γ is the Gamma function and D_ν can be expressed with Kummer's confluent
 317 hypergeometric function of first kind [40], eq. 9.240, page 1028. This expression
 318 is valid if $-\alpha < p < 1/\xi$.

319 **Appendix B Pareto Tail for Meta-Gaussian**
 320 **Models**

Proposition 1. *Let Z be any positive absolutely continuous random variable with pdf f_Z and with a Pareto survival function \bar{F}_Z . Let X be any standardized normal distributed random variable, and let us define the positive random variable*

$$Y \stackrel{d}{=} \psi(X),$$

where $\stackrel{d}{=}$ means equality in distribution and $\psi(\cdot)$ represents a continuous and increasing function from the real line to $[0, \infty)$. The two random variables Z and Y are tail-equivalent if and only if

$$\lim_{x \rightarrow \infty} \frac{x\psi(x)}{\psi'(x)} = \frac{1}{\xi}, \quad (\text{B1})$$

321 where ξ corresponds the common positive GP shape parameter of Z .

322 **Proof of Proposition 1:** Let ϕ and $\bar{\Phi}$ denote respectively the pdf and
 323 survival function of a standard normal distribution X .

Recall that Z and Y are tail-equivalent, if and only

$$\lim_{y \rightarrow \infty} \frac{\bar{F}_Z(y)}{\mathbb{P}[Y > y]} = c \in (0, \infty),$$

This condition is satisfied if they have the same tail index. Assuming a Pareto tail with positive shape parameter ξ for Z implies that Z is regularly varying with index $1/\xi$. Proposition A.3.8(b) from [41] recalled that this regular variation type is equivalent to

$$\lim_{z \rightarrow \infty} \frac{z \times f_Z(z)}{\bar{F}_Z(z)} = \frac{1}{\xi}.$$

Hence, to show that Y and Z are tail equivalent, one needs to determine under which condition it can be written that

$$\lim_{z \rightarrow \infty} \frac{z \times F(z)}{\bar{F}_Y(z)} = \frac{1}{\xi}.$$

324 where f and \bar{F} denote the pdf and survival function of Y , respectively.
 By construction, the survival function of Y equals to

$$\bar{F}_Y(z) = \mathbb{P}[X > \psi^{-1}(z)] = \bar{\Phi}[\psi^{-1}(z)],$$

The density of Y is

$$f(z) = (\psi^{-1}(z))' \phi[\psi^{-1}(z)].$$

Then one can write

$$\frac{z \times f(z)}{\bar{F}_Y(z)} = \left(z \times \psi^{-1}(z) \times (\psi^{-1}(z))' \right) \times \left(\frac{\phi[\psi^{-1}(z)]}{\psi^{-1}(z) \bar{\Phi}[\psi^{-1}(z)]} \right).$$

Mill's ratio [41] tells us that the ratio in the last bracket goes to one as $\psi^{-1}(z)$ goes to ∞ (i.e. as z grows). Hence, the condition

$$\lim_{z \rightarrow \infty} \left(z \times \psi^{-1}(z) \times (\psi^{-1}(z))' \right) = \frac{1}{\xi}, \quad (\text{B2})$$

is equivalent to

$$\lim_{z \rightarrow \infty} \frac{z \times f(z)}{\bar{F}_Y(z)} = \frac{1}{\xi}.$$

325 This is equivalent to have tail equivalence between Z and Y .

326 Changing variables with $z = \psi(x)$, $x = \psi^{-1}(z)$ and $(\psi^{-1}(z))' = dx/dz$,
327 condition (B2) is equivalent to condition (B1).

328 This is the necessary and sufficient condition on $\psi(\cdot)$ to build a Pareto
329 random variable of tail index ξ from a standardized normal random variable
330 X .

331 **Acknowledgments.** The authors acknowledge Météo France for the data
332 sets.

333 This work was supported by Eau du Ponant SPL, and took place in the
334 context of the MEDISA (Méthodologie de Dimensionnement des Systèmes
335 d'Assainissements) project.

336 Part of P. Naveau's work work was supported by the French national pro-
337 gram (80 PRIME CNRS-INSU), and the European H2020 Xaida (Grant
338 agreement ID: 101003469). The author also acknowledges the support of the
339 French Agence Nationale de la Recherche (ANR) under reference ANR-20-
340 CE40-0025-01 (T-REX project), and the ANR-Melody (ANR-19-CE46-0011)

341 .

342 References

- 343 [1] Bauer, P., Thorpe, A., Brunet, G.: The quiet revolution of numerical
344 weather prediction. *Nature* **525**(7567), 47–55 (2015)
- 345 [2] Caseri, A., Javelle, P., Ramos, M.-H., Leblois, E.: Generating precipitation
346 ensembles for flood alert and risk management. *Journal of Flood Risk
347 Management* **9**(4), 402–415 (2016)
- 348 [3] Katz, R.W.: Extreme value theory for precipitation: sensitivity analysis
349 for climate change. *Advances in water resources* **23**(2), 133–139 (1999)

350 [4] Wilks, D.S.: Interannual variability and extreme-value characteristics
351 of several stochastic daily precipitation models. *Agricultural and forest*
352 *meteorology* **93**(3), 153–169 (1999)

353 [5] Castellvi, F., Mormeneo, I., Perez, P.: Generation of daily amounts of
354 precipitation from standard climatic data: a case study for argentina.
355 *Journal of hydrology* **289**(1-4), 286–302 (2004)

356 [6] Shoji, T., Kitaura, H.: Statistical and geostatistical analysis of rainfall in
357 central japan. *Computers & Geosciences* **32**(8), 1007–1024 (2006)

358 [7] Woolhiser, D.A., Roldan, J.: Stochastic daily precipitation models: 2. a
359 comparison of distributions of amounts. *Water resources research* **18**(5),
360 1461–1468 (1982)

361 [8] Liu, Y., Zhang, W., Shao, Y., Zhang, K.: A comparison of four precipi-
362 tation distribution models used in daily stochastic models. *Advances in*
363 *Atmospheric Sciences* **28**(4), 809–820 (2011)

364 [9] Hussain, I., Spöck, G., Pilz, J., Yu, H.-L.: Spatio-temporal interpolation
365 of precipitation during monsoon periods in pakistan. *Advances in water*
366 *resources* **33**(8), 880–886 (2010)

367 [10] Guillot, G., Lebel, T.: Disaggregation of sahelian mesoscale convec-
368 tive system rain fields: Further developments and validation. *Journal of*
369 *Geophysical Research: Atmospheres* **104**(D24), 31533–31551 (1999)

370 [11] Allcroft, D.J., Glasbey, C.A.: A latent gaussian markov random-field
371 model for spatiotemporal rainfall disaggregation. *Journal of the Royal*
372 *Statistical Society: Series C (Applied Statistics)* **52**(4), 487–498 (2003)

373 [12] Allard, D., Bourotte, M.: Disaggregating daily precipitations into hourly
374 values with a transformed censored latent gaussian process. *Stochastic*
375 *environmental research and risk assessment* **29**(2), 453–462 (2015)

376 [13] Maraun, D., Wetterhall, F., Ireson, A., Chandler, R., Kendon, E., Wid-
377 mann, M., Brienen, S., Rust, H., Sauter, T., Themeßl, M., et al.:
378 Precipitation downscaling under climate change: Recent developments to
379 bridge the gap between dynamical models and the end user. *Reviews of*
380 *Geophysics* **48**(3) (2010)

381 [14] Rebora, N., Ferraris, L., von Hardenberg, J., Provenzale, A.: Rain-
382 farm: Rainfall downscaling by a filtered autoregressive model. *Journal of*
383 *Hydrometeorology* **7**(4), 724–738 (2006)

384 [15] Zhao, T., Bennett, J.C., Wang, Q., Schepen, A., Wood, A.W., Robertson,
385 D.E., Ramos, M.-H.: How suitable is quantile mapping for postprocessing

20 *A meta-Gaussian distribution for sub-hourly rainfall*

386 gcm precipitation forecasts? *Journal of Climate* **30**(9), 3185–3196 (2017)

387 [16] Sigrist, F., Künsch, H.R., Stahel, W.A., *et al.*: A dynamic nonstationary
388 spatio-temporal model for short term prediction of precipitation. *The
389 Annals of Applied Statistics* **6**(4), 1452–1477 (2012)

390 [17] Benoit, L., Allard, D., Mariethoz, G.: Stochastic rainfall modeling at sub-
391 kilometer scale. *Water Resources Research* **54**(6), 4108–4130 (2018)

392 [18] Bardossy, A., Plate, E.J.: Space-time model for daily rainfall using atmo-
393 spheric circulation patterns. *Water resources research* **28**(5), 1247–1259
394 (1992)

395 [19] Ailliot, P., Thompson, C., Thomson, P.: Space-time modelling of pre-
396 cipitation by using a hidden markov model and censored gaussian
397 distributions. *Journal of the Royal Statistical Society: Series C (Applied
398 Statistics)* **58**(3), 405–426 (2009)

399 [20] Kleiber, W., Katz, R.W., Rajagopalan, B.: Daily spatiotemporal precipi-
400 tation simulation using latent and transformed gaussian processes. *Water
401 Resources Research* **48**(1) (2012)

402 [21] Lien, G.-Y., Kalnay, E., Miyoshi, T.: Effective assimilation of global pre-
403 cipitation: Simulation experiments. *Tellus A: Dynamic Meteorology and
404 Oceanography* **65**(1), 19915 (2013)

405 [22] Li, W., Duan, Q., Ye, A., Miao, C.: An improved meta-gaussian distri-
406 bution model for post-processing of precipitation forecasts by censored
407 maximum likelihood estimation. *Journal of Hydrology* **574**, 801–810
408 (2019)

409 [23] Cecinati, F., Wani, O., Rico-Ramirez, M.A.: Comparing approaches to
410 deal with non-gaussianity of rainfall data in kriging-based radar-gauge
411 rainfall merging. *Water Resources Research* **53**(11), 8999–9018 (2017)

412 [24] Box, G.E., Cox, D.R.: An analysis of transformations. *Journal of the Royal
413 Statistical Society: Series B (Methodological)* **26**(2), 211–243 (1964)

414 [25] Panofsky, H.A., Brier, G.W., Best, W.H.: Some Application of Statistics to
415 Meteorology. *Earth and Mineral Sciences Continuing Education, College
416 of Earth and . . . , ???* (1958)

417 [26] Wilks, D.: Multisite generalization of a daily stochastic precipitation
418 generation model. *Journal of Hydrology* **210**(1-4), 178–191 (1998)

419 [27] Papalexiou, S., Koutsoyiannis, D., Makropoulos, C.: How extreme is
420 extreme? an assessment of daily rainfall distribution tails. *Hydrology &*

421 Earth System Sciences **17**(1) (2013)

422 [28] Katz, R.W., Parlange, M.B., Naveau, P.: Statistics of extremes in
423 hydrology. *Advances in water resources* **25**(8-12), 1287–1304 (2002)

424 [29] Furrer, E.M., Katz, R.W.: Improving the simulation of extreme precipita-
425 tion events by stochastic weather generators. *Water Resources Research*
426 **44**(12) (2008)

427 [30] Baxevani, A., Lennartsson, J.: A spatiotemporal precipitation generator
428 based on a censored latent gaussian field. *Water Resources Research*
429 **51**(6), 4338–4358 (2015)

430 [31] Naveau, P., Huser, R., Ribereau, P., Hannart, A.: Modeling jointly low,
431 moderate, and heavy rainfall intensities without a threshold selection.
432 *Water Resources Research* **52**(4), 2753–2769 (2016)

433 [32] Tencaliec, P., Favre, A.-C., Naveau, P., Prieur, C., Nicolet, G.: Flexible
434 semiparametric generalized pareto modeling of the entire range of rainfall
435 amount. *Environmetrics* **31**(2), 2582 (2020)

436 [33] Tukey, J.W.: Modern techniques in data analysis. In: *Proceedings of the*
437 *NSF-Sponsored Regional Research Conference*, vol. 7 (1977). Southern
438 Massachusetts University

439 [34] Goerg, G.M.: The lambert way to gaussianize heavy-tailed data with the
440 inverse of tukey'sh transformation as a special case. *The Scientific World*
441 *Journal* **2015** (2015)

442 [35] Xu, G., Genton, M.G.: Tukey g-and-h random fields. *Journal of the*
443 *American Statistical Association* **112**(519), 1236–1249 (2017)

444 [36] Ribereau, P., Naveau, P., Guillou, A.: A note of caution when interpreting
445 parameters of the distribution of excesses. *Advances in Water Resources*
446 **34**(10), 1215–1221 (2011)

447 [37] Coles, S.G., Dixon, M.J.: Likelihood-based inference for extreme value
448 models. *Extremes* **2**(1), 5–23 (1999)

449 [38] Carreau, J., Naveau, P., Neppel, L.: Partitioning into hazard subregions
450 for regional peaks-over-threshold modeling of heavy precipitation. *Water*
451 *Resources Research* **53**(5), 4407–4426 (2017)

452 [39] Vannitsem, S., Naveau, P.: Spatial dependences among precipitation max-
453 ima over belgium. *Nonlinear Processes in geophysics* **14**(5), 621–630
454 (2007)

455 [40] Gradshteyn, I.S., Ryzhik, I.M.: Table of Integrals, Series, and Products,

22 *A meta-Gaussian distribution for sub-hourly rainfall*

456 7th edn. Academic press, ??? (2007)

457 [41] Embrechts, P., Klüppelberg, C., Mikosch, T.: Modelling Extremal Events:
458 for Insurance and Finance vol. 33. Springer, ??? (2013)